



An Efficient Hybrid Approach Model for SARS-CoV-2 Prediction Using an Optimized Deep Learning Recurrent Neural Network and Fuzzy inference

Zaid Dereaa¹, Ammar Kazm², Jasim Mohammed Atyiah³, Oday Ali Hassen^{2,4,*},
Esraa Saleh Alomari²

¹College of Computer Science and Information Technology, Wasit University, Iraq

²Department of Computer, College of Education for Pure Sciences, Wasit University, Iraq

³College of Islamic Sciences, Department of Islamic Creed and Thought, Samarra University, Iraq

⁴Ministry of Education, Wasit Education Directorate, Wasit, Iraq

Emails: zabdulameer@uowasit.edu.iq; aawaad@uowasit.edu.iq; Presidency@uosamarra.edu.iq;
odayali@uowasit.edu.iq; ealomari@uowasit.edu.iq

Abstract

SARS-CoV2 virus has affected the peoples in worldwide with several issues, like health and economy. Moreover, mathematical definition of fractal dimension affords a method for calculating the non-linear dynamic behaviour difficulty revealed through time series of countries. The fuzzy logic model illustrates and manages the characteristic uncertainty of classification issue. In this paper, an effectual SARS-CoV2model is developed using optimized Deep learning model through time series data. The derived features are derived from the input sequential data for disease forecasting. Moreover, over sampling scheme is exploited for data augmentation, which enhances the prediction process. Fuzzy systems and various distance measures are calculated for choosing most significant features. The Deep Recurrent Neural network (DRNN) is applied for performing SARS-CoV2prediction, in which DRNN is trained through designed Fractional Water Poor and Rich Optimization (FrWPRO) method. Meanwhile, the training process of DRNN using hybrid optimization model from scratch proves that, the designed SARS-CoV2prediction method accomplishes better performance compared to other existing approaches with Mean Square Error (MSE), Root MSE (RMSE), and Mean Absolute Percentage Error (MAPE) of 0.1425, and 0.3775, and 0.3467 respectively.

Keywords: Fuzzy inference; Deep learning; Weighted Moving Average; Time series data; Lee distance

1. Introduction

Coronavirus 2019, named as SARS-CoV2epidemic was spread from Wuhan, China to other countries in worldwide. It has huge pathological contamination and also quick rate of spread, while compared with preceding infectious diseases [9]. SARS-CoV2disease has encountered people in worldwide with various issues because of its emergence. Moreover, it has more harmful influences on interrupted economy and people's health. Therefore, various countries have employed strong interferences for controlling the disease spread and also decreases the negative effects of SARS-CoV2disease [10] [1]. The biological model of SARS-CoV2comprises positive sense single standard RNA typical that is more complex for identifying disease due to the mutation power. Besides, SARS-CoV2may produce various severe problems for humans

and it has more complexity in multi organ failure, pneumonia, sudden cardiac arrest, multi organ failure and breathing [11]. The medical professionals exist in the world carry out more serious research in order to familiarize effective treatment process for SARS-CoV2[12]. Several efficient control measures are executed, such as travel restriction, social distancing, traffic control, environmental disinfection, online working, wearing of mask, target isolation, delaying of work resumption and so on [2]. The most imperative ways for maintaining the virus spread is isolation, sanitization, social distancing, masking, and utilization of scientific schemes without the physical contacts. The prediction and identification of spread pattern based on scientific approaches are useful for framing the policies as well as outbreak containing [7]. Generally, time series analysis was performed for prediction process in which various elements are essential for analysis. Various time series data has seasonality, trend, and irregularity related to them. Furthermore, some of these elements are performed in cyclic order, although it is not essential to perform time series model form.

It is critical to include database stationarity in order to predict time series analysis. Time series data to be stationary, and it more indispensable for analysis in addition, it has three elements, such as autocovariance, constant variance and mean, which does not rely on time [5]. Furthermore, autoregression is fundamentally a time series method it uses the observations from preceding time steps as input to any regression expression to predict the importance of next time step. This procedure is simple, that consequences the precise prediction on specified range of time series issues. Commonly, machine learning and data mining approaches are utilized in order to predict the SARS-CoV2disease [13] [14] [15] and the data is gathered and processed from various sources in secured manner [16] [6]. Additionally, fluctuation is a time series behaviour it can be employed for evaluating the pattern, as well as prediction process. Moreover, fuzzy time series is more expressive, while compared with conventional time series, since it affords semantic meaning for fluctuating and uncertain data [7]. There is an extensive type of techniques in order to calculate fractal dimension generating a crisp rate through time series data for specific issue. This value affords an evaluation of difficulty of a certain time series data. The fuzzy values for fractal dimensions are formulated as well as fuzzy rules along with the capability to categorize the countries depends on SARS-CoV2based on the range of crisp rates for fractal dimension evaluations [17] [8].

In modern days, various deep learning algorithms, namely Convolutional Neural networks (CNN) and attention methods have attained promising outcomes in various regions, like stock market price prediction, and Natural Language Processing (NLP) and etc [1] rather than Long Short-Term Memory (LSTM) method. Moreover, the improved technique was employed to predict SARS-CoV2for performing swab test and also observe the biotic material collected from patients through RT-PCR. However, it is more challenging process, wherein swab assessment is considered for covid affected persons. Currently, Artificial Intelligence (AI) is most commonly utilized approach for fastening bio-medical researchers [12]. Furthermore, major machine learning technique application for automatic prediction in medical areas is more effective and also it is efficient tool for doctors [19] [20]. Deep learning outperforms conventional analysis and machine classification approaches on large and diverse datasets [21] [18] and demonstrates the use of several deep learning algorithms used previously, but it will be applied in more healthcare domains in the future to increase diagnostic quality. Additionally, deep learning method is more familiar research area of AI and it enables end to end approaches in order to attain efficient outcome using input image. The deep learning methods are utilized to solve various problems, like breast cancer, lung cancer, skin cancer, brain cancer classifications, arrhythmia prediction, pneumonia detection, and fundus image segmentation. In addition, Gray Level Co-occurrence Matrix (GLCM) was utilized in [22] to extract hand-crafted features. Furthermore, feature set was exploited to automatic identification of SARS-CoV2identification along with residual exemplar Local Binary Pattern (LBP) approach through chest X-ray image [23].

The main contribution of this research:

The major intention of this research is to design an effectual SARS-CoV2prediction approach using time series data with optimization driven deep learning. In this research, time series data is considered for predicting the covid-19. Moreover, technical indicator extraction is most imperative process in order to perform prediction process. Distance measures and fuzzy systems are exploited for choosing imperative features, then data augmentation is carried out for improving prediction performance. In addition, DRNN is applied for predicting covid-19, and the DRNN is trained by proposed optimization method, named Fr-WPRO technique.

1.1 State of art methods

Various SARS-CoV2prediction approaches are designed by researchers in past few years, although eight papers are reviewed here. Abbasimehr, H. and Paki, R., [1] designed combination of deep learning schemes and Bayesian optimization for SARS-CoV2prediction. Here, several deep learning systems, namely Long Short-Term Memory (LSTM), multi-head attention, and Convolutional Neural Network (CNN) were employed with optimization algorithm. The Bayesian optimizer chooses the hyperparameters, thereby the performance was increased. However, this way did

not derive more effectual indicators. Niu, Y.S., *et al.* [2] modelled Spatio-Temporal Neural Network (STNN) for prediction of covid-19. The variants of STNN were trained by means of Stochastic Gradient Descent (SGD) model. In this method, computational and training performance was reduced, although it needs more training data for processing. Babukarthik, R.G., *et al.* [3] developed Genetic Deep learning CNN (GDCNN) for the prediction of covid-19. This prediction model attained improved nominal rate for disease detection even in unbalanced model. Although, this method did not employ huge size dataset in order to attain better classification accuracy. Alazab, M., *et al.* [4] introduced deep CNN for SARS-CoV2 prediction using chest images. The system price was minimal and it attained better performance precision. Even though, it failed to evaluate the terrain effects of temperature, humidity.

Chyon, F.A., *et al.* [5] presented Autoregressive Integrated Moving Average (ARIMA) method for SARS-CoV2 prediction. This system was the incorporation of various stochastic process utilized for assessing the time series data. This approach was more reliable, but it did not utilize less variance data for improving accuracy of prediction. Namasudra, S., *et al.* [6] designed Nonlinear Autoregressive (NAR) model for SARS-CoV2 prediction. This approach was trained using network configuration parameters and training models for avoiding overfitting issues. However, this prediction approach failed to reduce computational time. Kumar, N. and Susan, S., [7] introduced Particle Swarm Optimization (PSO) technique for prediction of covid-19. Here, nested Fuzzy Time Series (FTS) as well as exhaustive search model in order to identify the optimal interval length and also the fuzzy order Cao., *et al.* [12]. Here, outer PSO model optimizes the number of partitions for decreasing the price whereas inner PSO optimizes boundaries of intervals. The running time was reduced in this system, even though it did not consider other circumstances of covid-19. Castillo, O. and Melin, P., [8] designed Intelligent Fuzzy Fractal technique for SARS-CoV2 prediction. Here, the fuzzy system was included for classification process. This technique has minimal computational time, although decision making process was not effective for classification process.

1.2 Challenges

The difficulties experienced by the existing techniques are explicated as follows,

- Deep learning methods with optimization was introduced in [1] for SARS-CoV2 prediction, but it failed to extract more efficient features in order to enhance the system performance.
- In [3], GDCNN model was introduced for SARS-CoV2 prediction, even though it failed to utilize huge database for enhancing the accuracy of classification.
- ARIMA technique was designed for prediction of SARS-CoV2 in [5], although did not explore various prediction methods, like Bayesian networks, artificial neural network (ANN), and Support Vector Machines (SVM) in order to improve system performance.
- In [6], NAR scheme was developed for predicting covid-19, however it did not include activation functions and training techniques, thereby performance was reduced.
- Intelligent Fuzzy Fractal method was devised in [8] for predicting covid-19, even though it did not incorporate various neural networks, such as ensemble and self-organizing techniques for analyzing temporal and spatial patterns.

2. Data specification

Novel Coronavirus (COVID-19) cases data [24] is utilized for the implementation of proposed prediction approach. This database is section of SARS-CoV2 contagion, which is collected for Engineering by Johns Hopkins University centre and system science from other various sources. Additionally, this database encompasses different areas; like region/country, recovered, suspected, confirmed, deaths, last updated, and province/state fields. Here, whole amount of rows as well as attributed exist in death, confirmed cases, percentage of death and confirmed is 277 and 513. Besides, the rows and columns of recovered percentage and cases are 513 and 263.

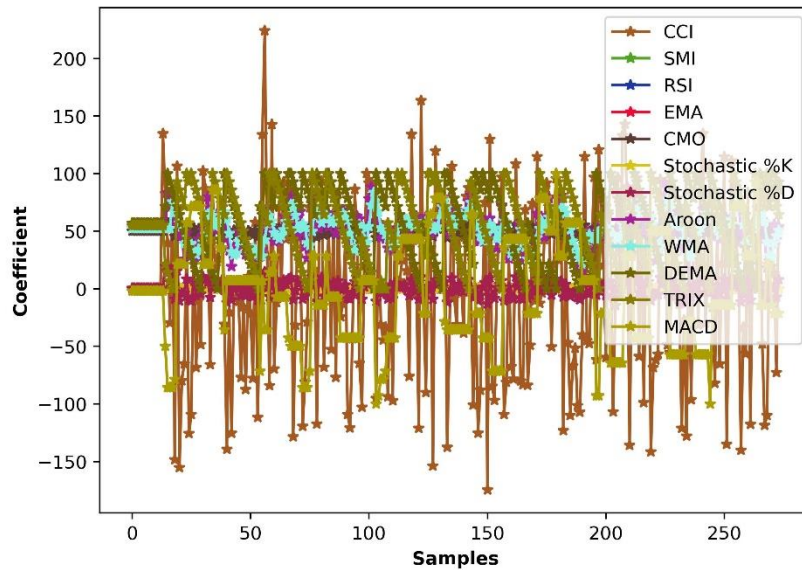


Figure 1. Data distribution plot

3. Time series modelling

Generally, time series is vector series it is illustrated as $s(j)$, wherein j specifies elapsed period. Let us consider, the scalar series for easiness, although the considered methods generalize readily to vector sequence. In theoretic cases, s has the rate of constantly varying with j similar to temperature. The term s is sampled for formulating discrete data series points, which are equally spaced in time for any physical system during the practical way. Besides, the samples generate maximum resolution, even though high resolution is not have optimal predictive power, thus appropriate outcome is obtained by considering every v^{th} point in a sequence.

The function of Neural Network (NN) is majorly focused on further progression of time series prediction from the rate of s until the present duration. Therefore, identify the function $h : \hat{h}^N \rightarrow \hat{h}$ for detecting the rate of s at time $j + t$ from N time steps back from instance j , thereby,

$$s(j + t) = e(s(j), s(j - 1), \dots, s(j - N + 1)) \tag{1}$$

where, $s(j + t) = e(y(j))$, where $s(j)$ denotes N-ary vector of lagged s values. Commonly, t is one, so e predicts the next s rate.

4. CT predict modelling

An effectual SARS-CoV2time series prediction approach using time series data is devised and it is explained in this section. This technique mainly includes four stages, includes the measure derivation mechanism, selection the features, Data expansion and and SARS-CoV2 Forecasting. Initially, input time series data is forwarded to technical indicator extraction module in which the features, like Commodity Channel Index (CCI), Stochastic Momentum Index (SMI), Relative Strength Index (RSI), Exponential Moving Average (EMA), Chande’s Momentum Oscillator (CMO), Stochastic %K, Aroon indicator [25],Stochastic %D, Weighted Moving Average (WMA),Triple Exponential Average(TRIX) Moving Average Convergence Divergence (MACD) are extracted, Double Exponential Moving Average (DEMA). Once the technical indicator is extracted, the features are selected based on fuzzy and distance measures, like Levenshtein distance, Lee distance, Jaro–Winkler distance, and Hamming distance. After that, data augmentation is done in order to

enhance the dimension of data. Finally, SARS-CoV2 is predicted based on Deep Recurrent Neural Network (Deep RNN) [26], which is trained using the proposed optimization algorithm, named Fractional Water Poor and Rich Optimization (FrWPRO). The FrWPRO is designed newly by integrating Water Cycle Algorithm (WCA) [27], Poor and Rich Optimization (PRO) [28] along with Fractional Calculus [29]. The diagram of introduced SARS-CoV2 prediction model is displayed in figure 1.

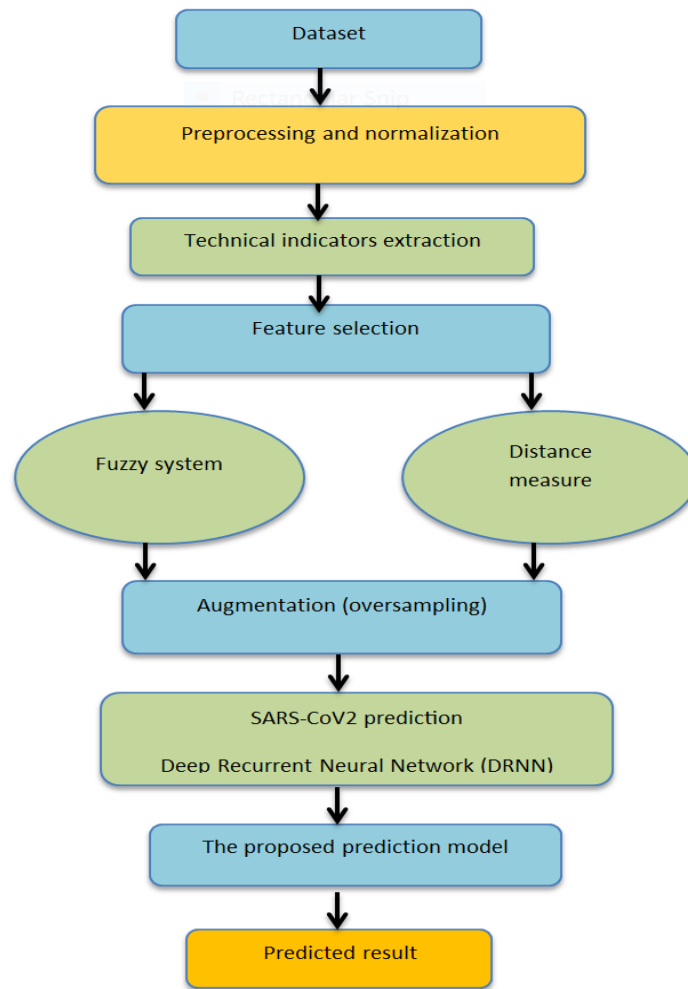


Figure 2. Block representation of SARS-CoV2 prediction model

4.1 Input time series data

Usually, time series data is a sequence of data points indexed in period order and it is used for predicting the imminent patterns or trends with historical database by means of technical features. Hence, to predict SARS-CoV2 time series data is considered for that, the time series dataset F with z amount of time series data, it is expressed as,

$$F = \{F_1, F_2, \dots, F_r, \dots, F_v\} \tag{2}$$

Where, v refers total amount of time series data, and F_r designates r^{th} index of data in a dataset.

4.2 Extraction of time-based feature indicators

The time series data F_r is taken from a dataset for extracting technical features, which is used for prediction. Usually, technical indicators exploit the technical rules, which depends on historical data over certain time instance for predicting future value by means of mathematical operations. Various technical features extracted from input time series data is explicated as below.

4.2.1 CCI

Usually, the oscillator is employed for finding whether the data is low or high, even though it specifies the relationship between data. It is evaluated by,

$$C_1 = \frac{O - M}{(0.015 \times R)} \tag{3}$$

where,

$$O = \frac{X + T + E}{3} \tag{4}$$

Here, X symbolizes high data, T denotes minimal data, E implies closing value, M is n period moving average of O, and R is absolute rate mean deviation of difference among mean value and its moving average.

4.2.2 SMI

It is computed by means of low and high values, which is specified by,

$$D_2 = 100 \times \left(\frac{2E_n}{X_n - T_n} \right) \tag{5}$$

where, E_n is closest data in day n , T_n depicts high data in day n , and X_n specifies lowest data on day n .

4.2.3 RSI

This feature compares the current minimal rate with highest value for representing weakness ort strength of data rate, which is estimated by,

$$D_3 = 100 - \frac{100}{1 + N} \tag{6}$$

where, N is ratio of smoothed n average period gains divided by absolute rate of smoothed n period average losses.

4.2.4 EMA

It is referred as moving average class, which includes weight rate for the estimation of future rate, and it is expressed as,

$$D_4 = \sum_{k=0}^{p-1} Q_k E_{n-k} \tag{7}$$

where, E represents weight.

4.2.5 CMO

It is estimated based on the difference among negative and positive directional movement, and it is evaluated by,

$$D_5 = 100 \times \frac{K(q^+) - K(q^-)}{K(q^+) + K(q^-)} \tag{8}$$

where, K symbolizes Simple Moving Average (SMA), q^+ denotes positive directional movement, and q^- is negative directional movement.

4.2.6 Stochastic %K

It is utilized for verifying the amount of data over the period of n days, which is illustrated by,

$$D_6 = 100 \times \frac{E_n - X_n}{X_n - T_n} \tag{9}$$

4.2.7 Stochastic %D

This indicator affords turnaround signal denotation, which specifies the infected cases is overbought and overrated. It is estimated as 3-days of stochastic %K attained over a time of n prior days similar to input window length. It is calculated as,

$$D_7 = 100 \times \left(\frac{E - A_{14}}{L_{14} - A_{14}} \right) \tag{10}$$

4.2.8 Aroon indicator

This feature [25] is utilized for finding trend variations in a data with regards to period, which is estimated by,

$$D_8 = T_{up} - T_{down} \tag{11}$$

where,

$$T_{up} = 100 \times \frac{25 - L_{25}}{25} \tag{12}$$

$$T_{down} = 100 \times \frac{25 - A_{25}}{25} \tag{13}$$

where, L_{25} implies high data since 25 days time, and A_{25} symbolizes low data since 25 days period.

4.2.9 WMA

This technical feature is estimated through providing weight to particular time and this element locates more importance on present and previous data. In this indicator, every period of data is multiplied by weight and it is detected by amount of selected time period. This technical indicator is symbolized as D_9 .

4.2.10 DEMA

This technical indicator is defined as a rate of SARS-CoV2 to afford more weight to present time period. Additionally, it is more responsive for the variations in Covid-19, and it is estimated by,

$$D_{10} = (2 \times D_4(y) - D_4(D_4(y))) \tag{14}$$

where, D_4 indicates EMA, and y signifies time period.

4.2.11 TRIX

It is utilized for smoothing the irrelevant SARS-CoV2 predictions, and it is expressed by,

$$D_{11} = \frac{x(H)}{x(H-1)} \tag{15}$$

where, x indicates triple moving rate and H implies exponential moving average.

4.2.12 MACD

This technical feature activates several data, when it crosses below and above the time series data, and it is represented as D_{12} .

Moreover, extracted technical indicators from input data is deliberated by below expression,

$$D = \{D_k\} ; k = 1,2,\dots,12 \tag{16}$$

where, D denotes extracted technical indicator.

4.3 Feature selection based on fuzzy and distance measures

The extracted technical indicators D is considered for feature selection process, wherein features are chosen based on various distance measures and fuzzy system.

For each technical features, Levenstein, Lee, Jaro-winkler and hamming distances are computed among target and feature, thereby four values are generated.

a) Levenstein distance: This metric is utilized for measuring the difference among two data. The Levenstein distance is calculated by following expression,

$$Lev_{a,b}(i, j) = \begin{cases} \max(i, j) & ; \text{if } (\min(i, j)) = 0 \\ \min \begin{cases} Lev_{a,b}(i-1, j) + 1 \\ Lev_{a,b}(i, j-1) + 1 \\ Lev_{a,b}(i-1, j-1) + 1 \end{cases} & ; \text{Otherwise} \end{cases} \tag{17}$$

Here, i refers candidate feature, j implies previous feature and levenstein distance is denoted as S_j .

b) Lee distance: This distance is estimated based on the distance among two data, it is assessed by following equation.

$$Lee(x_i, x_j) = \sum_{y=1}^n \min(|x_i - x_j|, q - |x_i - x_j|) \tag{18}$$

Here, the Lee distance is specified by S_{Lee} .

c) Jaro-winkle distance: This distance is a variant of Jaro distance measure, which is an edit distance amongst two sequences. It is evaluated by below equation,

$$SW = S_j + P * L * (1 - S_j) \tag{19}$$

where, SW indicates Jaro-winkle similarity among candidate and previous feature, P is scaling factor, L signifies length of matching prefix, S_j specifies Jaro-winkle similarity among candidate and target feature, and S_j is Jaro-winkle measure.

d) Hamming distance: The hamming distance between features are computed by,

$$D_H = \sum_{i=1}^K |x_i - y_i| \tag{20}$$

Here, for every features, four values are produced based on the above distance measures and the produced values are subjected as input to fuzzy system.

e) Fuzzy system

The Genetic Fuzzy System (GFS) [30] is commonly a fuzzy system, which is augmented through the learning process by means of Genetic Algorithm (GA). The fuzzy models specify the capability for solving various types of issues in application area. The adaptive GFS model is employed to optimize the membership functions and rules. Figure 3 displayed the model of fuzzy system.

In general, adaptive GFS has following phases, creation of rules from data and applying GA for elaborating exploration issues. The formulation of simple approach to the scheme of discretization and membership function. The last final phase is development of fitness measure through permitting frequency of rules occurrence in training data. Here, the fuzzy score is computed for every feature and then set the threshold rate. After that, choose the features, which has higher fuzzy score than threshold rate.

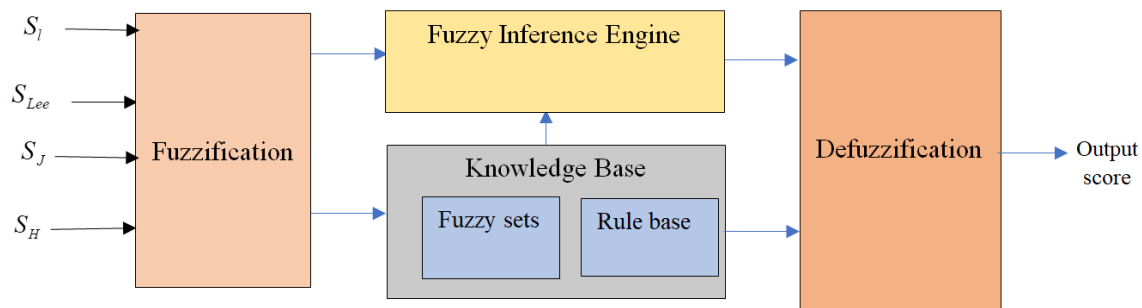


Figure 3. Fuzzy system

Therefore, the outcome of feature selection is denoted as V , and it is augmented for improving performance.

4.4 Data augmentation to strengthen DRNN training

The selected features V is considered as input for augmentation, in which oversampling model is applied. It enlarges the data size without including other additional data, hence SARS-CoV2 prediction performance is highly enhanced. The over sampling model divided the data according to the class labels. The maximum and less values are selected from every label and also it formulates residual samples. The chosen data size is $d \times c$, and it is incremented as $k \times c$, wherein d is incremented to k using over sampling technique. Hence, data augmented outcome is denoted as B and it is used for further prediction process.

4.5 Devised SARS-CoV2 prediction using Fractional Water Poor and Rich Optimization-based DRNN

The augmented output B is fed as input to DRNN for predicting SARS-CoV2 and training process is carried out for improving prediction performance.

i) DRNN architecture

The DRNN [26] model is an Artificial Neural Network (ANN) with various amount of hidden layers as well as it records the dynamic network time series through directional connection of nodes at hidden layer. Moreover, it is totally different from Feed Forward Neural Network (FFNN), since it records the input series at various time states based on feedback and also feed forward associates between internal processing layers. Generally, DRNN is more robust variation of technical features and thus, it significantly improves the prediction ability. It is encompassing of various non-linear layers with regards to period. Although, the location of hidden layer is position efficacy of prior hidden layer and it is vertical expansion over instance. Every series of data is efficiently estimated as well as present outcome is exploited for predicting future outcome rate. Moreover, it utilizes the random sequence information and it employed the historical data at restricted amount of stages. It maps the input series to hidden states, then it is employed for mapping output based on feature learning. The hidden layer process is expressed by,

$$W_p = g(BY^{WB} + W_{p-1}Y^{WW}) \tag{21}$$

where, W_{p-1} is prior hidden state, g represents non-linear function, Y specifies weight factor, Y^{WW} implies weight element, Y^{WB} refers weight between input and hidden layer. Furthermore, input processing element is recorded in internal state through activation function and the output estimated in output layer is specified as,

$$M = g(W_p Y^{MW}) \tag{22}$$

where, M denotes output, and Y^{MW} indicates weight between output and hidden layer. Figure 4 sows the structure of DRNN.

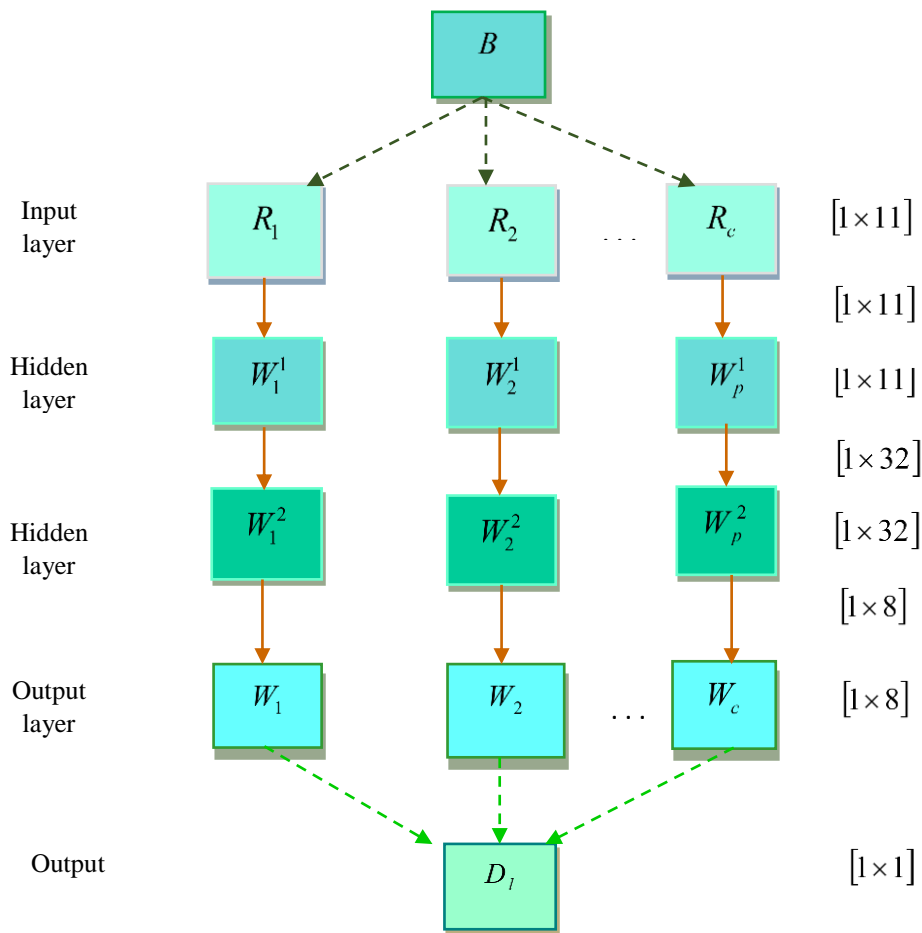


Figure 4. DRNN structure

ii) Training algorithm-Fractional Water Poor and Rich Optimization technique

An effectual optimization approach, named FrWPRO method is introduced to train DRNN, which improves the prediction effectiveness. PRO technique [28] is designed by the stimulation of dual sets of populations, namely rich and poor. The poor people try to attain wealth and dimmish class gap, while rich peoples accomplish wealth and also improve their gap in class. On the other hand, WCA [27] is mainly introduced by rivers towards sea, stream flow and water cycle observation. Moreover, the fractional concept is also incorporated for enhancing the better performance.

Solution encoding

It is an illustration of solution that depicts the evaluation of optimal solution for weight element at every iteration of optimization along with fitness function. The solution dimension is specified as $U = 1 \times Q$, in which optimal rate for weight Q is assessed through optimization scheme.

i) Initialization

The initial population is formulated randomly along with equal distribution according to upper and lower bound parameters. Then, arrange the initial population in ascending order through including objective function. The population in the optimization model is group of dual subpopulations, like poor and rich in search space (C). The population is represented as,

$$K_{op} = K_{poor} + K_{rich} \tag{23}$$

where, K_{op} refers main population, K_{poor} implies poor population, and K_{rich} indicates rich population.

ii) Fitness value estimation

The fitness measure us used for finding optimal solution, wherein the fitness with least error rate is considered as best solution for prediction.

$$F_p = \frac{1}{t} \sum_{f=1}^t [D_f - M_f]^2 \tag{24}$$

where, F_p designates fitness measure, D_f signifies target outcome, t refers whole amount of training samples.

iii) Update the location of rich populations

The location of member in rich population for all iteration by means of WPRO approach is expressed as,

$$\overrightarrow{G_{rich,w}^{new}} = \frac{1 - rand H}{rand H + l} \left[\frac{rand H G_{sea}^w (1 + l)}{1 - rand H} + l \overrightarrow{G_{poor,best}^{old}} \right] \tag{25}$$

In order to apply fractional calculus subtract $\overrightarrow{G_{rich,w}^{old}}$ on both sides,

$$\overrightarrow{G_{rich,w}^{new}} - \overrightarrow{G_{rich,w}^{old}} = \frac{1 - rand H}{rand H + l} \left[\frac{rand H G_{sea}^w (1 + l)}{1 - rand H} + l \overrightarrow{G_{poor,best}^{old}} - \overrightarrow{G_{rich,w}^{old}} \right] \tag{26}$$

Let us consider,

$$\overrightarrow{G_{rich,w}^{new}} = G_{rich,w}^{(l+1)} \tag{27}$$

$$\overrightarrow{G_{rich,w}^{old}} = G_{rich,w}^{(l)} \tag{28}$$

$$\overrightarrow{G_{poor,best}^{old}} = G_{poor,best}^{(l)} \tag{29}$$

$$G_{rich,w}^{(l+1)} - G_{rich,w}^{(l)} = \frac{1 - rand H}{rand H + l} \left[\frac{rand H G_{sea}^w (1 + l)}{1 - rand H} + l G_{poor,best}^{(l)} - \overrightarrow{G_{rich,w}^{(l)}} \right] \tag{30}$$

Apply fractional calculus on above equation,

$$D^p [G_{rich,w}^{(l+1)}] = \frac{1 - rand H}{rand H + l} \left[\frac{rand H G_{sea}^w (1 + l)}{1 - rand H} + l G_{poor,best}^{(l)} - \overrightarrow{G_{rich,w}^{(l)}} \right] \tag{31}$$

$$G_{rich,w}^{(l+1)} - pG_{rich,w}^{(l)} - \frac{1}{2} pG_{rich,w}^{(l-1)} - \frac{1}{6} (1-p)G_{rich,w}^{(l-2)} + \frac{1}{24} p(1-p)(2-p)G_{rich,w}^{(l-3)} = \frac{1-rand H}{rand H + l} \left[\frac{rand H G_{sea}^w (1+l)}{1-rand H} + lG_{poor,best}^{(l)} - \overrightarrow{G_{rich,w}^{(l)}} \right] \tag{32}$$

$$G_{rich,w}^{(l+1)} = G_{rich,w}^{(l)} (p-1) + \frac{1}{2} pG_{rich,w}^{(l-1)} + \frac{1}{6} (1-p)G_{rich,w}^{(l-2)} + \frac{1}{24} p(1-p)(2-p)G_{rich,w}^{(l-3)} + \frac{1-rand H}{rand H + l} \left[\frac{rand H G_{sea}^w (1+l)}{1-rand H} + lG_{poor,best}^{(l)} \right] \tag{33}$$

where, $\overrightarrow{G_{rich,w}^{old}}$ refers present value of w^{th} place, *rand* denotes arbitrary integer, which lies amongst $[0,1]$, $\overrightarrow{G_{rich,w}^{new}}$ symbolizes new rate of w^{th} location in rich population, *a* indicates class gap parameter ranges from $[0,1]$, and *A* signifies parameter, which comprises the rate of $[1,2]$.

iv) Evaluate the mutation

The mutation for rich and poor population is assessed based on mutation probability, it is expressed as,

$$\overrightarrow{G_{rich,w}^{new}} = \overrightarrow{G_{rich,w}^{new}} + q \tag{34}$$

$$\overrightarrow{G_{poor,w}^{new}} = \overrightarrow{G_{poor,w}^{new}} + q \tag{35}$$

where, $\overrightarrow{G_{poor,w}^{new}}$ is mutation rate of poor population, $\overrightarrow{G_{rich,w}^{new}}$ implies mutation value of rich population, and *q* denotes normal distribution of mean rate as 0 and variance of 1.

v) Update equation of poor population's

Finally, poor population is updated according to below equation,

$$\overrightarrow{G_{poor,w}^{new}} = \overrightarrow{G_{poor,w}^{old}} + \left[b \times W - \overrightarrow{G_{poor,w}^{old}} \right] \tag{36}$$

where, $\overrightarrow{G_{poor,w}^{new}}$ refers new rate of w^{th} place, *b* signifies improvement element of pattern, which lies from $[0,1]$, and $\overrightarrow{G_{poor,w}^{old}}$ depicts present value of w^{th} position.

$$W = \frac{\overrightarrow{G_{rich,best}^{old}} + \overrightarrow{G_{rich,mean}^{old}} + \overrightarrow{G_{rich,worst}^{old}}}{3} \tag{37}$$

where, $\overrightarrow{G_{rich,mean}^{old}}$ indicates average position, $\overrightarrow{G_{rich,best}^{old}}$ is best member of rich population, and $\overrightarrow{G_{rich,worst}^{old}}$ signifies position of worst member.

vi) Re-estimate the solution feasibility

Here, fitness value is assessed for each and every solution, wherein fitness with less value is taken as optimal solution.

5. Results and discussion

The outcomes of the designed SARS-CoV2 prediction system for various datasets are discussed in this section.

5.1 CT predict model-based time series analysis

Here, the results for time series analysis based on SARS-CoV2 prediction methods for various data are exposed in this section.

i) Death cases

Figure 5 shows the analysis of death cases using various approaches for different countries. The original death cases are 1606, while prediction result obtained by the other present methods, like GDCNN, DSPM, DNN, STNN, and WPRO-DRNN, and introduced Fr-WPRO enabled DRNN is 1671, 301, 696, 2134, 671, and 1698 as well as the error rate among original and GDCNN, DSPM, Deep NN, STNN, WPRO-based DRNN, and introduced Fr-WPRO scheme is 65, 1305, 910, 528, 935, and 92.

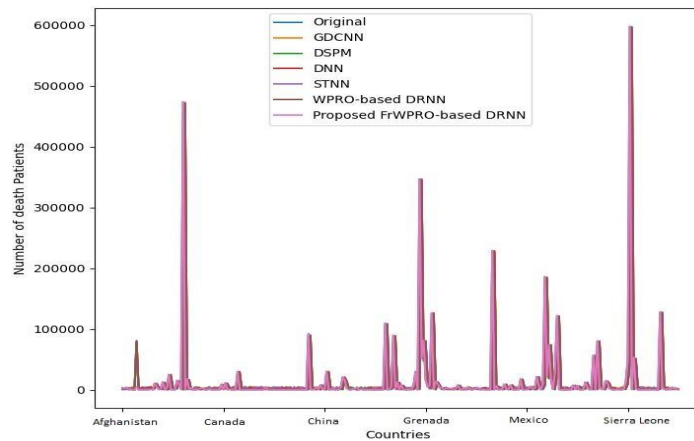


Figure 5. Analysis for death cases

ii) Infected cases

The analysis of infected cases based on several countries are exposed in figure 6. The original infected cases are 39189, and the existing methods and Fr-WPRO_DRNN are 76346, 29205, 89838, 32675, 2536, and 39243 and its error rate is 29890, 9984, 50649, 6514, 13829, and 54.

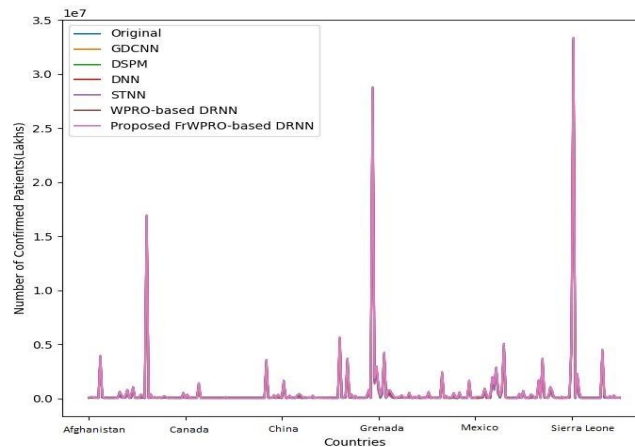


Figure 6. Analysis for infected cases

iii) Recovered cases

Figure 7 specifies the analysis of recovered cases by means of various approaches for diverse countries. The original death cases are 3571, when prediction result obtained by the other present methods, like GDCNN, DSPM, DNN, STNN, WPRO-DRNN, and developed Fr-WPRO enabled DRNN is 96429, 16356, 110791, 20643, 115933, and 3658 as well as the error rate among original and GDCNN, DSPM, Deep NN, STNN, WPRO-based DRNN, and introduced Fr-WPRO scheme is 92858, 12785, 107220, 17072, 112362, and 87.

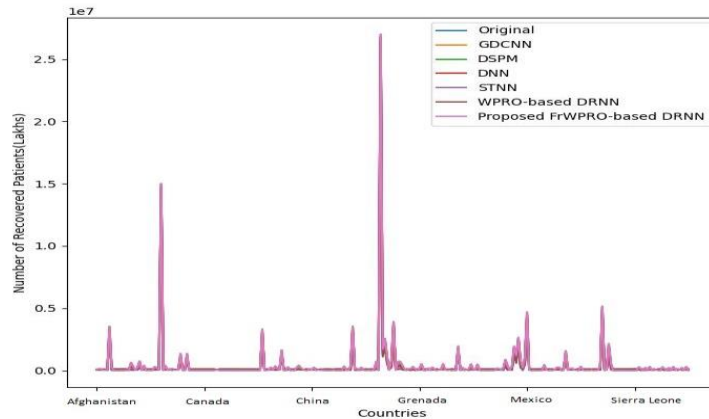


Figure 7. Analysis for recovered cases

iv) Percentage of confirmed cases

The analysis for percentage of confirmed cases based on several countries are exposed in figure 8. The original confirmed cases are 0.11746, and the existing methods and Fr-WPRO_DRNN are 0.2299, 0.0882, 0.2723, 0.0994, 0.0761, and 0.1176 and its error rate is 0.1125, 0.02920, 0.1549, 0.01801, 0.0413, and 0.00016.

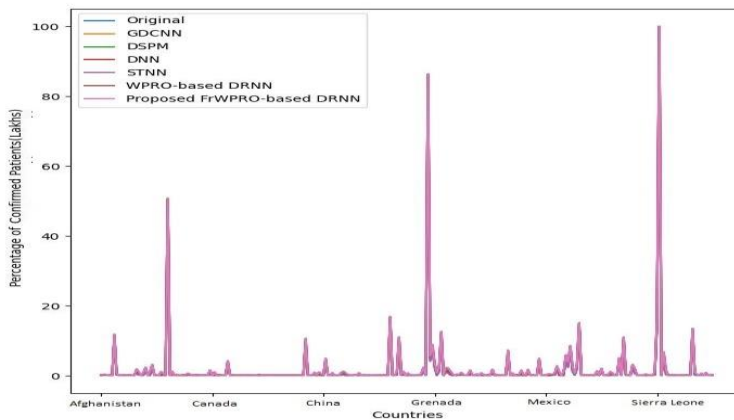


Figure 8. Analysis of confirmed cases

v) Percentage of death cases

Figure 9 specifies the analysis for percentage of death cases by means of various approaches for diverse countries. The original death cases are 0.26872, when prediction result obtained by the other present methods, like GDCNN, DSPM, DNN, STNN, WPRO-DRNN, and developed Fr-WPRO enabled DRNN is 0.2810, 0.0504, 0.1170, 0.35859, 0.11261, and 0.2840 as well as the error rate among original and GDCNN, DSPM, Deep NN, STNN, WPRO-based DRNN, and introduced Fr-WPRO scheme is 0.01231, 0.21832, 0.15168, 0.08986, 0.15611, and 0.01536.

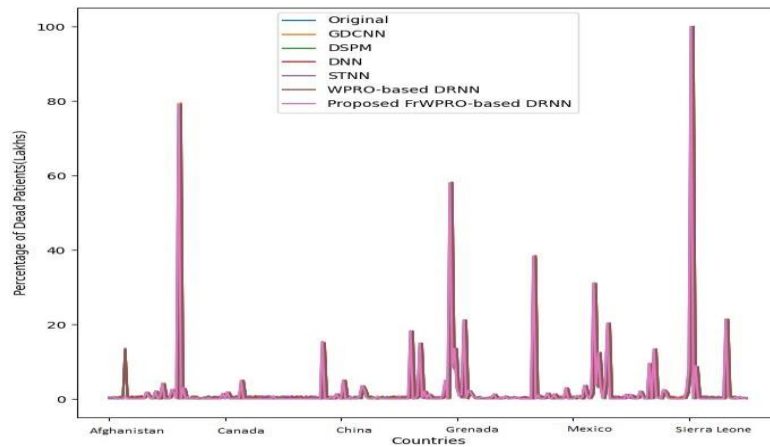


Figure 9. Death Cases Percentage Analysis

vi) Recovered Cases

The analysis for percentage of recovered cases based on several countries are exposed in figure 10. The original recovered cases are 0.01323, and the existing methods and Fr-WPRO_DRNN are 0.35867, 0.0611, 0.4158, 0.07786, 0.4394, and 0.01355 and its error rate is 0.3454, 0.0478, 0.4025, 0.0646, 0.4262, and 0.000322.

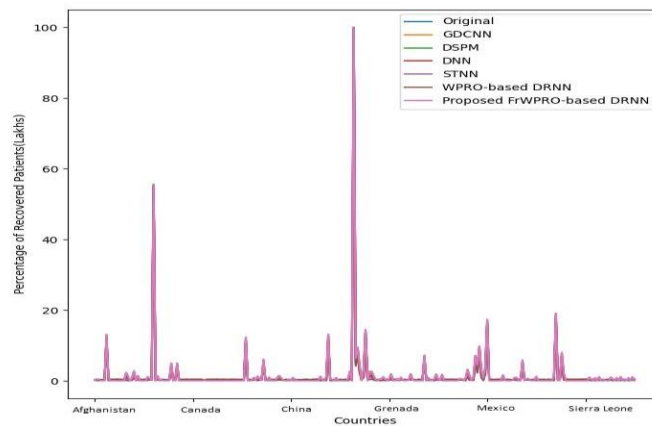


Figure 10. Analysis of recovered cases

5.3 Validation of CT predict model

Figure 11 represents the validation result for developed SARS-CoV2 approach, which contains validation and training loss. The validation loss is varied from 0.370006 to 0.012919, whereas training loss changes from 0.3852 to 0.02566 for iteration 0 to 300.

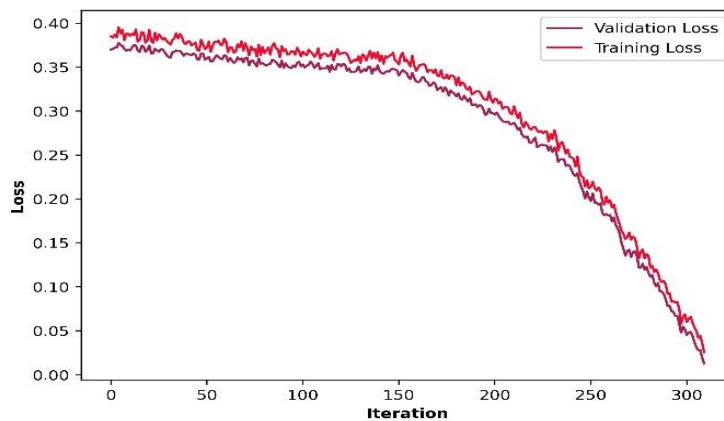


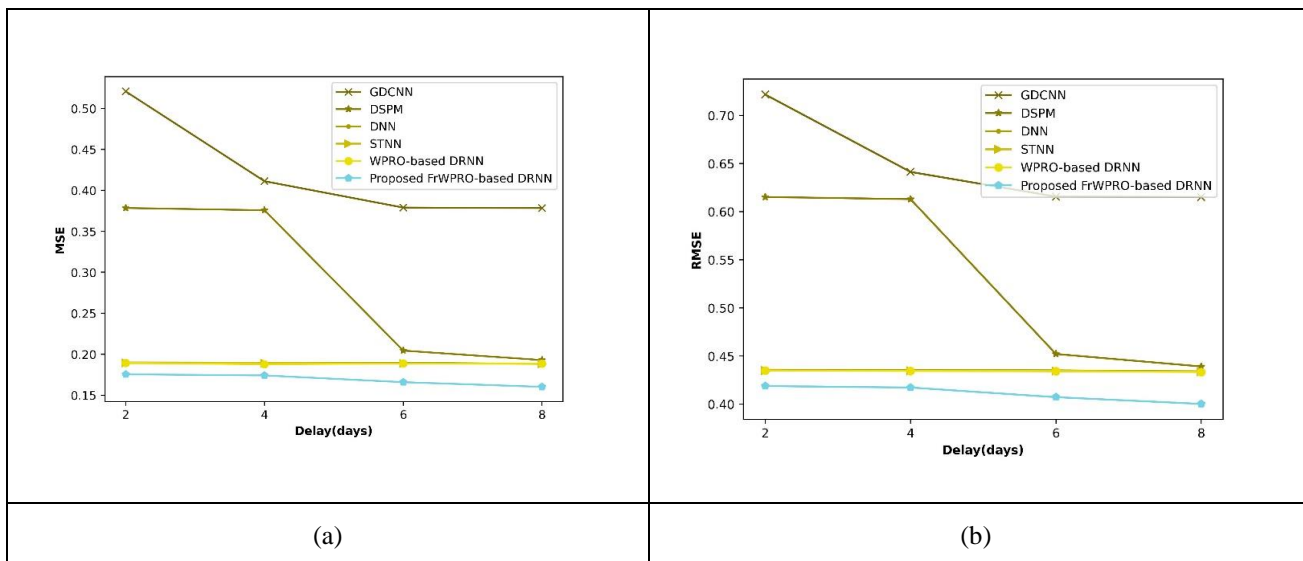
Figure 11. Validation analysis

5.4 Findings from validation of CT predict model

The major finding obtained for developed SARS-CoV2 method for various data with MSE, RMSE, and MAPE is specified in this section.

5.4.1 Analysis based on death case

Figure 13 depicts the analysis of devised Fr-WPRO-DRNN for death cases with regards to MSE and RMSE. While considering delay as 6, existing methods and Fr-WPRO driven DRNN is 0.3790, 0.2044, 0.1893, 0.1887, 0.1887, and 0.1658. Meanwhile, the RMSE of GDCNN is 0.61565, DSPM is 0.45214, DNN is 0.43509, STNN is 0.43440, WPRO_DRNN is 0.43435, and Fr-WPRO- DRNN is 0.40727. Moreover, the MAPE of GDCNN is 0.6078, DSPM is 0.5688, DNN is 0.507, STNN is 0.5255, WPRO_DRNN is 0.4866, and Fr-WPRO- DRNN is 0.4643 for delay 8.



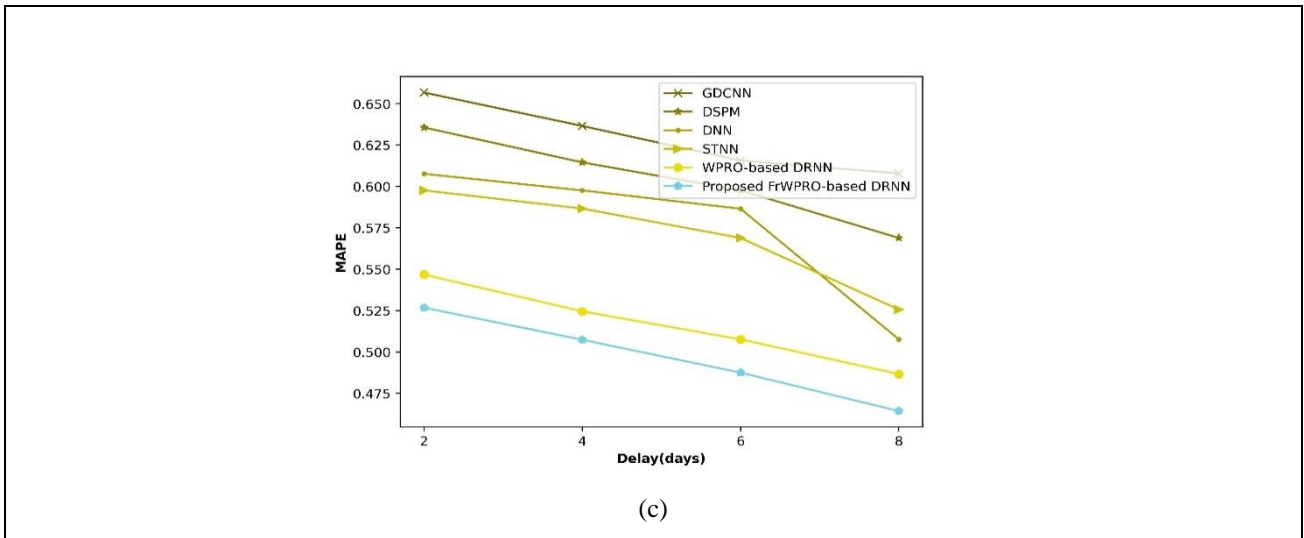
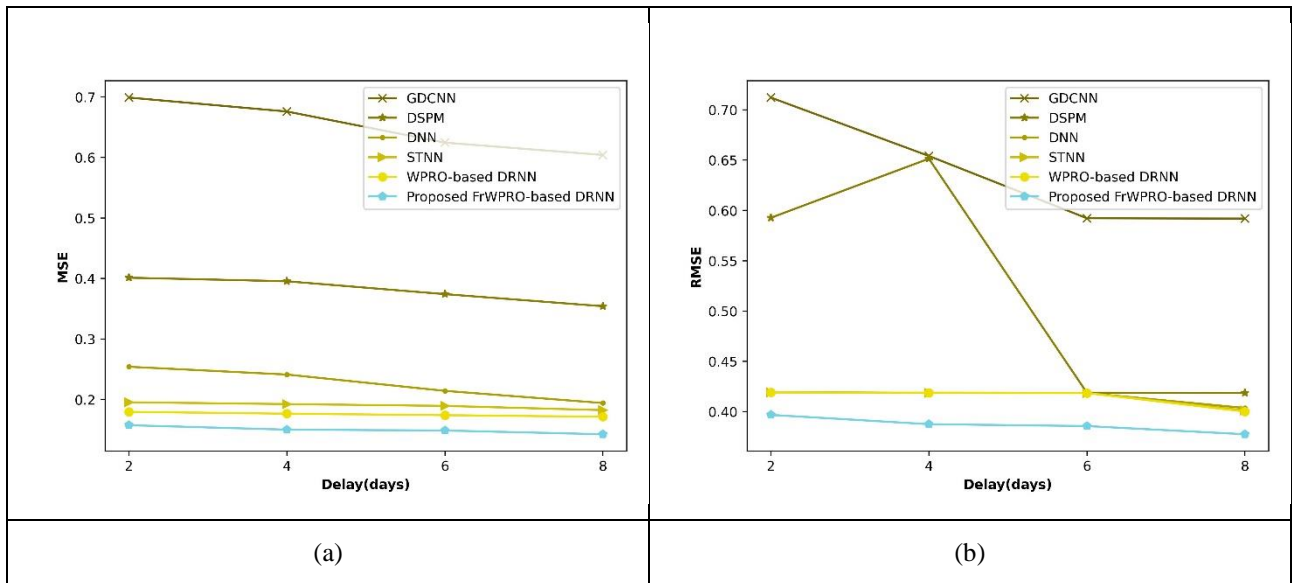


Figure 12. Comparative analysis of Fr-WPRO_DRNN for (a) MSE (b) RMSE and (c) MAPE

5.4.2 Analysis using confirmed cases

The analysis of Fr-WPRO-based DRNN using confirmed cases is illustrated in figure 13. The MSE of existing and developed Fr-WPRO-based DRNN is 0.6245, 0.3741, 0.2142, 0.1894, 0.1741, and 0.1487, whereas RMSE is 0.5922, 0.4187, 0.4185, 0.4185, 0.4185, and 0.3856 for delay 6. Moreover, the MAPE of GDCNN is 0.4976, DSPM is 0.4578, DNN is 0.4356, STNN is 0.4256, WPRO_DRNN is 0.3965, and Fr-WPRO- DRNN is 0.3467 for delay 8.



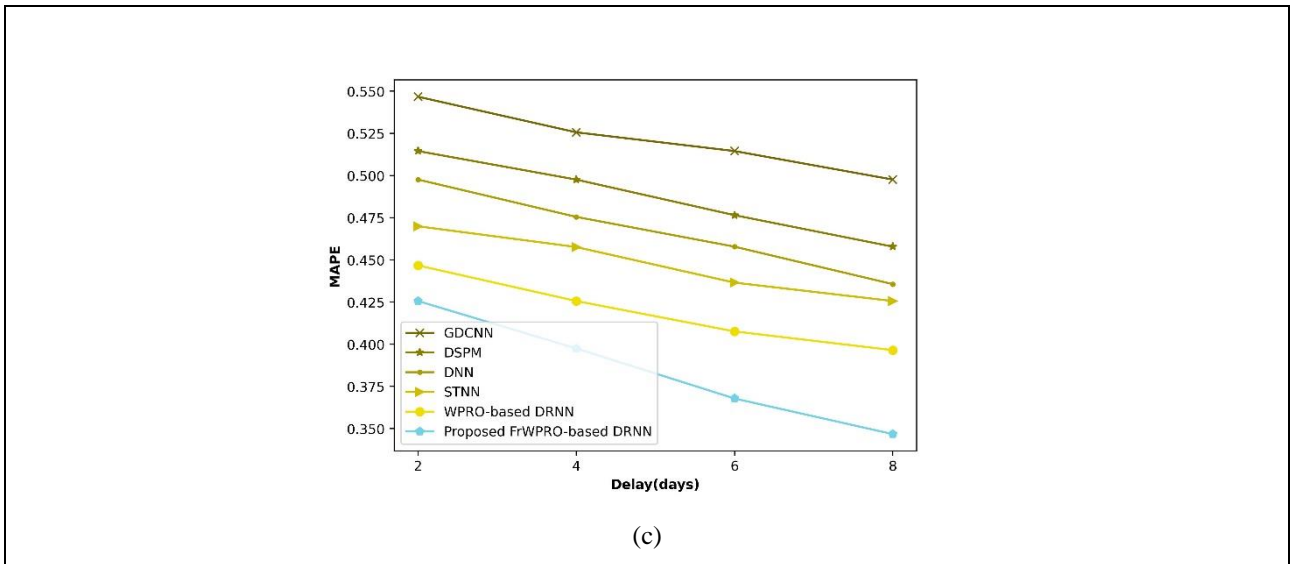
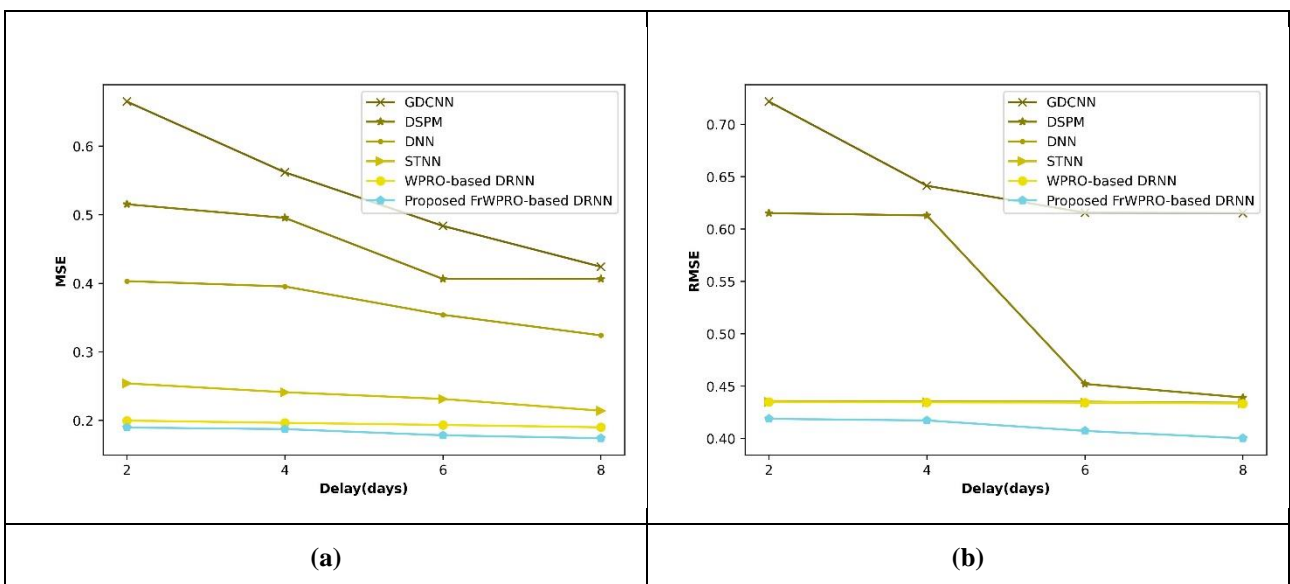


Figure 13. Comparative analysis of Fr-WPRO_DRNN for (a) MSE (b) RMSE and (c) MAPE

5.4.3 Recovered Cases Analysis

The analysis of Fr-WPRO driven DRNN for MSE and RMSE by changing delay is represented in figure 14. The MSE rate of GDCNN is 0.4836, DSPM is 0.40636, DNN is 0.35412, STNN is 0.23142, WPRO_DRNN is 0.19354, and Fr-WPRO- DRNN is 0.17845 in 6-delay rate. Besides, in 6 delay RMSE of existing and developed approaches are 0.6374, 0.4508, 0.45072, 0.4501, 0.4498, and 0.4224. Moreover, the MAPE of GDCNN is 0.5865, DSPM is 0.5543, DNN is 0.5356, STNN is 0.4876, WPRO_DRNN is 0.4756, and Fr-WPRO- DRNN is 0.4467 for delay 6.



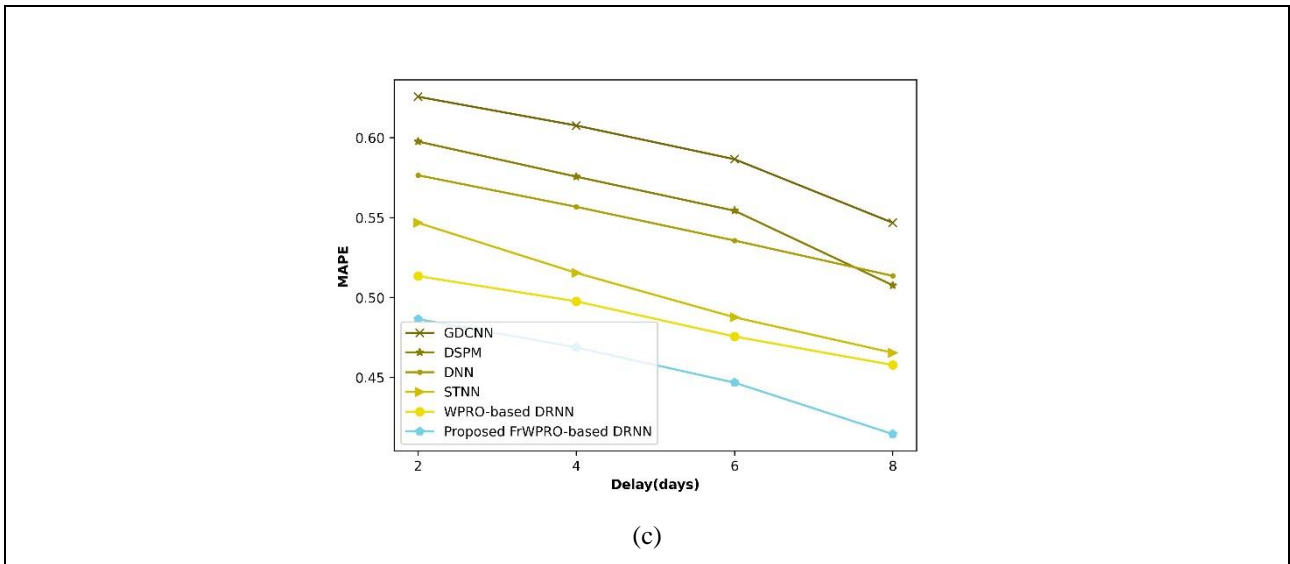
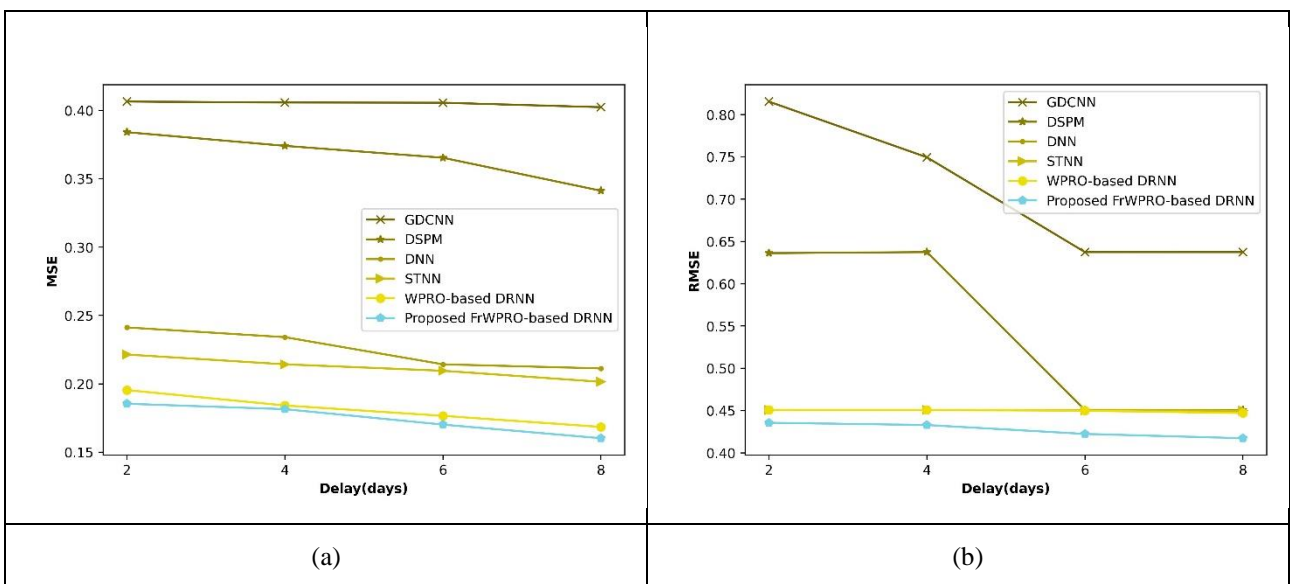


Figure 14. Comparative analysis of Fr-WPRO_DRNN for (a) MSE (b) RMSE and (c) MAPE

5.4.4 % of infection Analysis

Figure 13 depicts the analysis of devised Fr-WPRO-DRNN for death cases with regards to MSE and RMSE. While considering delay as 6, existing methods and Fr-WPRO driven DRNN is 0.4125, 0.3841, 0.29974, 0.2142, 0.19541, and 0.17001. Meanwhile, the RMSE of GDCNN is 0.6509, DSPM is 0.4701, DNN is 0.4641, STNN is 0.4535, WPRO_DRNN is 0.4215, and Fr-WPRO- DRNN is 0.4123. Moreover, the MAPE of GDCNN is 0.5976, DSPM is 0.5478, DNN is 0.5278, STNN is 0.5156, WPRO_DRNN is 0.4678, and Fr-WPRO- DRNN is 0.4365 for delay 8.



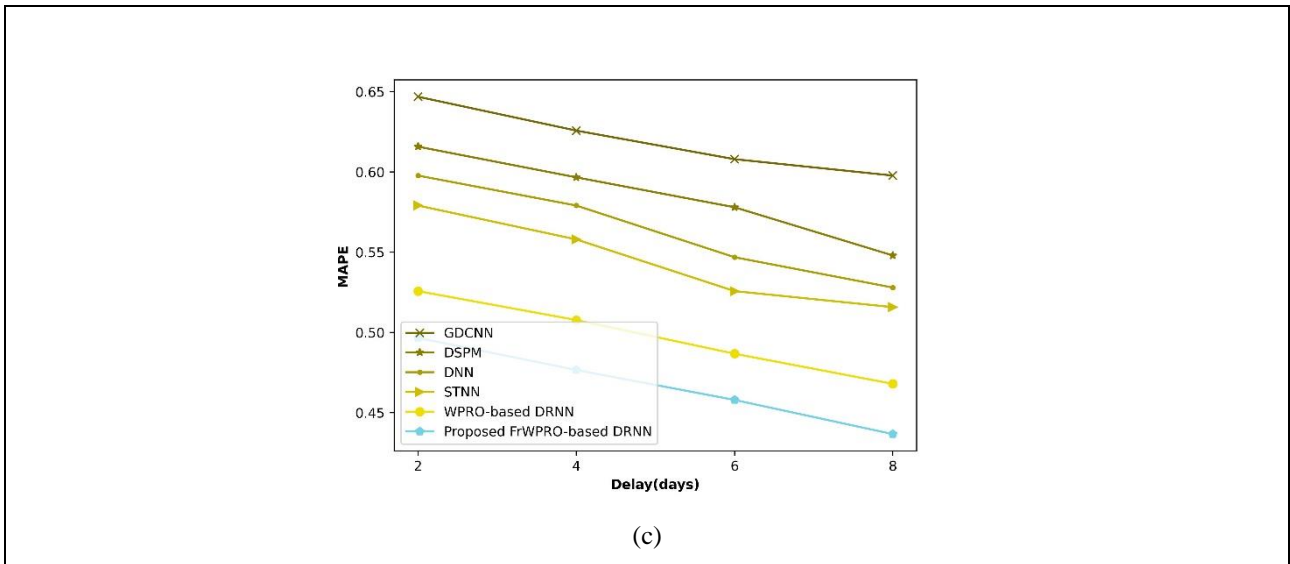
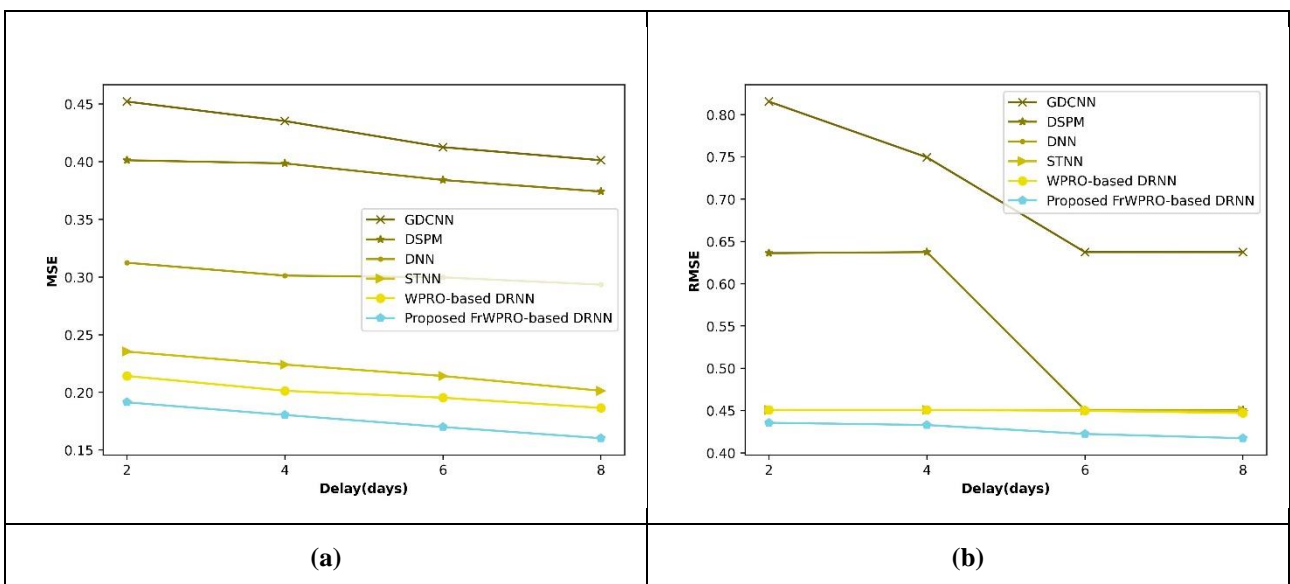


Figure 15. Comparative analysis of Fr-WPRO_DRNN for (a) MSE (b) RMSE and (c) MAPE

5.4.5 Analysis using % of death case

Figure 16 represents the analysis of devised Fr-WPRO-DRNN for percentage of death cases with regards to MSE and RMSE. While considering delay as 6, existing methods and Fr-WPRO driven DRNN is 0.4056, 0.3654, 0.2142, 0.2095, 0.1765, and 0.1701. Meanwhile, the RMSE of GDCNN is 0.6369, DSPM is 0.4526, DNN is 0.45080, STNN is 0.45037, WPRO_DRNN is 0.45037, and Fr-WPRO- DRNN is 0.4124. Moreover, the MAPE of GDCNN is 0.5577, DSPM is 0.5356, DNN is 0.4976, STNN is 0.4578, WPRO_DRNN is 0.4367, and Fr-WPRO- DRNN is 0.4245 for delay 8.



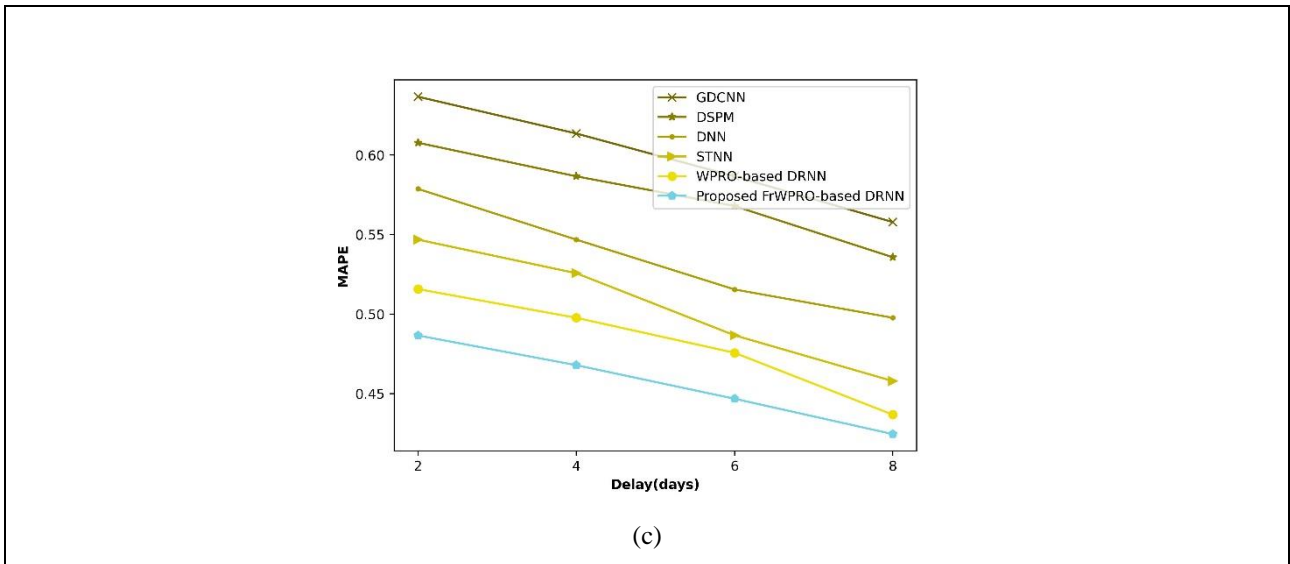
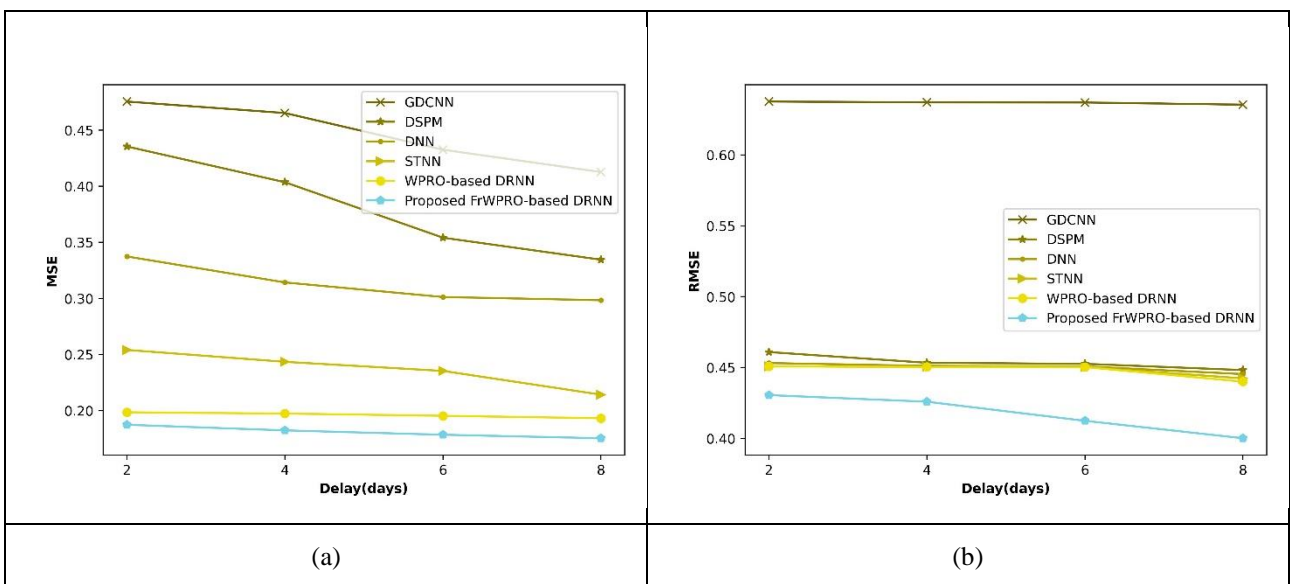


Figure 16. Comparative analysis of Fr-WPRO_DRNN for (a) MSE (b) RMSE and (c) MAPE

5.4.6 Analysis based on recovered case

The analysis of Fr-WPRO driven DRNN for MSE and RMSE by changing delay is represented in figure 17. The MSE rate of GDCNN is 0.43251, DSPM is 0.3541, DNN is 0.3012, STNN is 0.23541, WPRO_DRNN is 0.1954, and Fr-WPRO- DRNN is 0.1785 in 6 delay rate. Besides, in 6th delay RMSE of existing and developed approaches are 0.6035, 0.5974, 0.5965, 0.5841, 0.5824, and 0.4225. Moreover, the MAPE of GDCNN is 0.5578, DSPM is 0.5145, DNN is 0.4867, STNN is 0.4257, WPRO_DRNN is 0.4257, and Fr-WPRO- DRNN is 0.4177 for delay 6.



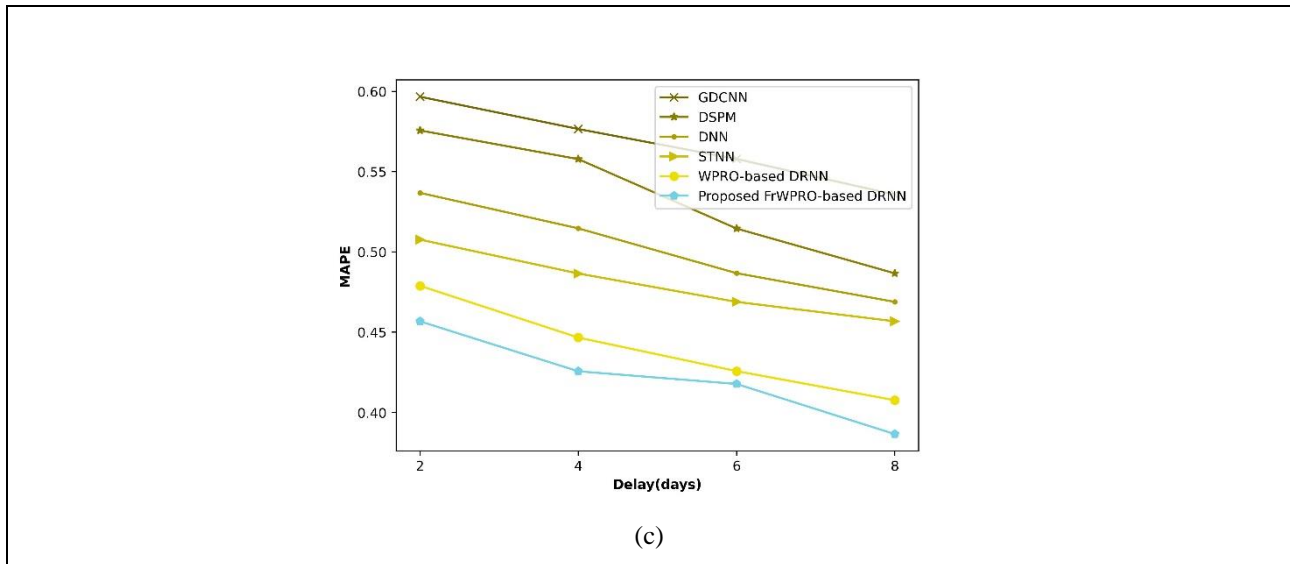


Figure 17. Comparative analysis of Fr-WPRO_DRNN for (a) MSE (b) RMSE and (c) MAPE

5.4.7 Discussion

The results obtained by proposed SARS-CoV2 prediction approach using time series data is discussed in this section. Table 3 explicates the comparative discussion of designed FrWPRO driven DRNN using death, confirmed, and recovered data with MSE, RMSE, and MAPE. While delay is 8, existing methods and Fr-WPRO driven DRNN is 0.3784, 0.1928, 0.1884, 0.1881, 0.1886, and 0.1602. Meanwhile, the RMSE of GDCNN is 0.6152, DSPM is 0.4391, DNN is 0.4341, STNN is 0.4337. WPRO_DRNN is 0.4334, [31],[32]. Fr-WPRO- DRNN is 0.4002. From the below table, it is deliberated that the developed FrWPRO_DRNN attained better performance with MSE of 0.1425 and RMSE of 0.3775 in confirmed case data.

Table 1: Comparative discussion for death, confirmed, and recovered data

Dataset	Methods / Metrics	GDCNN	DSPM	Deep NN	STNN	WPR-DRNN	Designed FrWPRO-based DRNN
Death case	MSE	0.3784	0.1928	0.1884	0.1881	0.1886	0.1602
	RMSE	0.6152	0.4391	0.4341	0.4337	0.4334	0.4002
	MAPE	0.6078	0.5688	0.507	0.525	0.4866	0.4643
Confirmed case	MSE	0.6041	0.3541	0.1941	0.1824	0.1714	0.1425
	RMSE	0.5918	0.4186	0.4036	0.4012	0.4001	0.3775
	MAPE	0.4976	0.4578	0.4356	0.4256	0.3965	0.3467
Recovered case	MSE	0.4241	0.4063	0.3241	0.2142	0.1901	0.1741
	RMSE	0.6374	0.4507	0.4498	0.4498	0.4471	0.4172
	MAPE	0.5865	0.5543	0.5356	0.4876	0.4756	0.4467

The comparative discussion of devised FrWPRO_DRNN based on percentage of death, confirmed, and recovered data with MSE and RMSE is shown in Table 4. The MSE of existing methods and Fr-WPRO_DRNN is 0.4024, 0.3412, 0.2112, 0.2014, 0.1684, and 0.1601, whereas RMSE of GDCNN is 0.6354, DSPM is 0.4482, DNN is 0.4454, STNN is 0.4424, WPRO_DRNN is 0.4401, and Fr-WPRO- DRNN is 0.4001. Moreover, the MAPE of GDCNN is 0.5578, DSPM is 0.5145, DNN is 0.4867, STNN is 0.4257,[33],[34]. WPRO_DRNN is 0.4257, and Fr-WPRO- DRNN is 0.4177. Thus, the proposed Fr-WPRO_DRNN obtained improved performance with MSE, RMSE, and MAPE of 0.160, 0.4001, and 0.4245 for percentage of death case.

Table 2: Comparative discussion for percentage of data

Dataset	Methods / Metrics	GDCNN	DSPM	DNN	STNN	WPR-DRNN	Designed FrWPRO-based DRNN
% of Death case	MSE	0.4024	0.3412	0.2112	0.2014	0.1684	0.1601
	RMSE	0.6354	0.4482	0.4454	0.4424	0.4401	0.4001
	MAPE	0.5577	0.5356	0.4976	0.4578	0.4367	0.4245
% of Confirmed case	MSE	0.4012	0.3741	0.2934	0.2014	0.1865	0.1602
	RMSE	0.6503	0.4701	0.4612	0.4501	0.4125	0.4003
	MAPE	0.5976	0.5478	0.5278	0.5156	0.4678	0.4365
% of Recovered case	MSE	0.4125	0.3345	0.2984	0.2142	0.1932	0.1754
	RMSE	0.5941	0.5841	0.5734	0.5654	0.5541	0.4188
	MAPE	0.5578	0.5145	0.4867	0.4257	0.4257	0.4177

6. Conclusion

This paper explicates an effectual SARS-CoV2prediction approach using optimized deep learning technique through time series data. The used dataset is taken from Novel SARS-CoV2 cases dataset. The input time series data is processed for extracting several technical indicators. Moreover, feature selection is carried out by means of various distance measures and fuzzy systems. The oversampling model is utilized for executing data augmentation process, thereby the prediction performance is improved by increasing the data size. The SARS-CoV2prediction process is done by means of DRNN classifier, and it is trained by designed FrWPRO technique. Based on the training process of deep learning the prediction performance is highly increased. Besides, the performance of proposed SARS-CoV2prediction model is evaluated by means of MSE and RMSE. The FrWPRO_DRNN model attained better performance with MSE, RMSE, and MAPE of 0.1425, 0.3775, and 0.3467 for confirmed cases, whereas the devised model attained the MSE, RMSE, and MAPE rate of 0.1601, 0.4001, and 0.4245 in percentage of death case. Further, the proposed SARS-CoV2prediction approach can be further improved by including other technical features. In addition, the processing time can be further decreased by considering other deep learning techniques.

References

- [1] H. Abbasimehr and R. Paki, "Prediction of SARS-COV2 confirmed cases combining deep learning methods and Bayesian optimization," *Chaos, Solitons Fractals*, vol. 142, 2021, Art. no. 110511.
- [2] Y.-S. Niu, W. Ding, J. Hu, W. Xu, and S. Canu, "Spatio-temporal neural network for fitting and forecasting COVID-19," *arXiv Prepr*, arXiv: 2103.11860, 2021.
- [3] R. G. Babukarthik, V. A. K. Adiga, G. Sambasivam, D. Chandramohan, and J. Amudhavel, "Prediction of SARS-COV2 using genetic deep learning convolutional neural network (GDCNN)," *IEEE Access*, vol. 8, pp. 177647–177666, 2020.
- [4] M. Alazab, A. Awajan, A. Mesleh, A. Abraham, V. Jatana, and S. Alhyari, "SARS-COV2 prediction and detection using deep learning," *Int. J. Comput. Inf. Syst. Ind. Manag. Appl.*, vol. 12, pp. 168–181, 2020.
- [5] F. A. Chyon, M. N. H. Suman, M. R. I. Fahim, and M. S. Ahmmed, "Time series analysis and predicting SARS-COV2 affected patients by ARIMA model using machine learning," *J. Virol. Methods*, vol. 301, 2022, Art. no. 114433.
- [6] S. Namasudra, S. Dhamodharavadhani, and R. Rathipriya, "Nonlinear neural network based forecasting model for predicting SARS-COV2 cases," *Neural Process. Lett*, pp. 1–21, Apr. 2021.
- [7] N. Kumar and S. Susan, "Particle swarm optimization of partitions and fuzzy order for fuzzy time series forecasting of COVID-19," *Appl. Soft Comput.*, vol. 110, 2021, Art. no. 107611.
- [8] O. Castillo and P. Melin, "A novel method for a SARS-CoV2 classification of countries based on an intelligent fuzzy fractal approach," *Healthcare*, vol. 9, no. 2, 2021, Art. no. 196.
- [9] İ. Kırbaş, A. Sözen, A. D. Tuncer, and F. Ş. Kazancıoğlu, "Comparative analysis and forecasting of SARS-COV2 cases in various European countries with ARIMA, NARNN and LSTM approaches," *Chaos, Solitons Fractals*, vol. 138, 2020, Art. no. 110015.
- [10] O. Torrealba-Rodriguez, R. A. Conde-Gutiérrez, and A. L. Hernández-Javier, "Modeling and prediction of SARS-COV2 in Mexico applying mathematical and computational models," *Chaos, Solitons Fractals*, vol. 138, 2020, Art. no. 109946.
- [11] F. Demir, "DeepCoroNet: A deep LSTM approach for automated detection of SARS-COV2 cases from chest X-ray images," *Appl. Soft Comput.*, vol. 103, 2021, Art. no. 107160.
- [12] J. Cao, X. Xu, Y. Wang, and H. Zhu, "Fuzzy inference system with interpretable fuzzy rules optimized by firefly algorithm for COVID-19 time series prediction," *Inf. Sci.*, vol. 660, pp. 119–135, 2024.
- [13] R. Sujath, J. M. Chatterjee, and A. E. Hassanien, "A machine learning forecasting model for SARS-COV2 pandemic in India," *Stoch. Environ. Res. Risk Assess*, vol. 34, no. 7, pp. 959–972, Jul. 2020.
- [14] Ali *et al.*, "DeepBalance: A deep reinforcement learning framework for dynamic load balancing in software-defined networks," *J. Intell. Syst. Internet Things*, vol. 17, no. 1, 2025.
- [15] M. John and H. Shaiba, "Main factors influencing recovery in MERS Co-V patients using machine learning," *J. Infect. Public Health*, vol. 12, no. 5, pp. 700–704, Sep. 2019.
- [16] S. Pradeepa *et al.*, "DRFS: Detecting risk factor of stroke disease from social media using machine learning techniques," *Neural Process. Lett*, pp. 1–19, Jun. 2020.
- [17] O. Castillo and P. Melin, "A new method for fuzzy estimation of the fractal dimension and its applications to time series analysis and pattern recognition," in *Proc. 19th Int. Conf. North Am. Fuzzy Inf. Process. Soc. (NAFIPS)*, 2000, pp. 451–455.
- [18] Utku, M. H. Sahin, and H. Ince, "Deep learning based hybrid prediction model for COVID-19 cross-country spread," *Expert Syst. Appl.*, vol. 228, 2023, Art. no. 120377.
- [19] S. R. Mohamedsaeed, A. K. Fakhrabadi, and M. S. Helfroush, "A novel deep learning approach for predicting COVID-19 severity using chest X-ray images," *Sci. Rep.*, vol. 12, no. 1, pp. 1–12, 2022.

- [20] H. Adhab, E. M. Kalik, and A. K. Al-Ani, "Designing a smart e-government application using a proposed hybrid architecture model dependent on edge and cloud computing," *Electron. Gov., Int. J.*, vol. 18, no. 3, pp. 340–353, 2022.
- [21] O. Faust *et al.*, "Deep learning for healthcare applications based on physiological signals: A review," *Comput. Methods Programs Biomed.*, vol. 161, pp. 1–13, 2018.
- [22] J. T. C. Ming *et al.*, "Lung disease classification using reticular pattern scoring and five class features with greedy stepwise based on GLCM," in *Proc. IEEE Region 10 Conf. (TENCON)*, 2017, pp. 182–186.
- [23] T. Tuncer, S. Dogan, and F. Ozyurt, "An automated residual exemplar local binary pattern and iterative ReliefF based SARS-COV2 detection method using chest X-ray image," *Chemometr. Intell. Lab. Syst.*, vol. 203, 2020, Art. no. 104054.
- [24] "Novel coronavirus (COVID-19) cases dataset," Hum. Data Exch., 2021. [Online]. Available: <https://data.humdata.org/dataset/novel-coronavirus-2019-ncov-cases>. Accessed: Oct. 2021.
- [25] K. Fakhrabadi, S. Hashemi, A. R. K. Khalilabad, and M. S. Helfroush, "A hybrid inception-dilated-ResNet architecture for deep learning-based prediction of COVID-19 severity," *Sci. Rep.*, vol. 15, no. 1, 2025, Art. no. 14032.
- [26] J. Cao, Y. Wang, and H. Zhu, "Enhanced prediction of COVID-19 cases using hybrid machine learning models," *Inf. Sci.*, vol. 660, pp. 119–135, 2024.
- [27] H. Eskandar, A. Sadollah, A. Bahreininejad, and M. Hamdi, "Water cycle algorithm—A novel metaheuristic optimization method for solving constrained engineering optimization problems," *Comput. Struct.*, vol. 110, pp. 151–166, 2012.
- [28] S. H. S. Moosavi and V. K. Bardsiri, "Poor and rich optimization algorithm: A new human-based and multi populations algorithm," *Eng. Appl. Artif. Intell.*, vol. 86, pp. 165–181, 2019.
- [29] P. R. Bhaladhare and D. C. Jinwala, "A clustering approach for the l -diversity model in privacy preserving data mining using fractional calculus-Bacterial," *Adv. Comput. Eng.*, vol. 2014, 2014, Art. no. 893198.
- [30] R. Rajeswari, P. Sudhakar, and V. Sugumaran, "FWLICM-Deep Learning: Fuzzy weighted local information C-means with RMDL for COVID-19 prediction using chest X-ray images," *J. Digit. Imag.*, vol. 35, pp. 1185–1198, 2022.
- [31] D. Ayris *et al.*, "A deep sequential prediction model (DSPM) to model and predict the COVID-19 outbreak," 2022.
- [32] M. Shanbehzadeh *et al.*, "Design of an artificial neural network to predict mortality risk due to COVID-19," 2022.
- [33] L. Xu *et al.*, "Forecasting COVID-19 new cases using deep learning methods (CNN, LSTM, CNN-LSTM)," *Comput. Biol. Med.*, vol. 144, 2022, Art. no. 105372.
- [34] D. Baihaqi, N. Yudistira, and E. Santoso, "Prediction of COVID-19 by Its Variants using Multivariate Data-driven Deep Learning Models," 2023.